Optimal Planning and Operation of Energy Storage Systems in Radial Networks for Wind Power Integration with Reserve Support

Mingwen Qin[1], *K. W. Chan*[1*], *C. Y. Chung*[2], *X. Luo*[1], *and Ting Wu*[1]

[1]*Department of Electrical Engineering, The Hong Kong Polytechnic University, Hong Kong, China*

[2]*Department of Electrical and Computer Engineering, University of Saskatchewan, Saskatoon, Canada*

[*]*corresponding author* eekwchan@polyu.edu.hk

Abstract: Though energy storage system (ESS) is a promising approach to alleviate the variability of non-dispatchable wind power and other forms of renewable energy sources, ~~However, the~~ its high investment cost ~~of ESS~~ has impeded ~~the~~ its widely deployment ~~of storage units~~. Aiming at exploiting the arbitrage benefit of ESS in reserve market and raising revenue of shareholders, this paper explores the optimal planning and operation of ESS in radial networks. Besides load balancing, ESS is used to provide three kinds of operating reserve ~~support~~ services in presence of high wind power penetration, including spinning reserve, upward and downward regulation reserves. In light of the capacity limitation of ESS, the time duration of reserve provision has been taken into account. In the proposed model, unit commitment and AC optimal power flow (AC-OPF) are combined together over sequential time series to find the optimal location and size of ESSs. In order to reduce the computational complexity, the extended *DistFlow* model of AC-OPF is adopted to convert the problem into a mixed-integer second-order cone programming ~~for efficient solution~~. Numerical studies on the IEEE 34-bus distribution test feeder ~~with various penetration levels of wind power and different scales of load~~ are used to investigate the effects of ESS with respect to various penetration levels of wind power and load scales.

Nomenclature

A. Indices and Sets

$\mathcal{N}$	Set of buses in the network.
$\mathcal{N}^s$	Set of substation buses in the network.
$\mathcal{L}$	Set of branches in the network.
ij	Branch between bus i and j, $(i,j) \in \mathcal{L}$.
$\mathcal{T}$	Sequential time series $\mathcal{T} = \{1,2,\ldots,T\}$.
$\mathcal{T}_0$	Sequential time series $\mathcal{T}_0 = \{0,1,2,\ldots,T\}$.
t	Time slot index.
Ω^r	Reserve category set $\Omega^r = \{sp, up, dw\}$.
k	Reserve category index $k \in \Omega^r$.

B. Parameters

T	Number of time slots.
Δt	Length of time interval in hours (typically 1 hr).
$\mathcal{R}_k$	Reserve demand of category $k \in \Omega^r$.
P_w	Forecast value of wind power.
$\tilde{P}_w$	Actual output of wind power.
δp	Wind disturbance reserve.
U^{ε}	Maximum number of buses for installing ESSs.
Cap^{ε}_{sum}	Total maximum power rating of energy reservoir capacity for all installed ESSs.
P_j^{ε,max_c}	Maximum active power production of ESS at bus j.
P_j^{ε,max_d}	Maximum active power consumption of ESS at bus j.

$Q_j^{\varepsilon,max}$ Maximum reactive power dispatching of ESS at bus j.

$S_j^{\varepsilon,max}$ Power capability limit of ESS at bus j.

$\eta_j^{in}, \eta_j^{out}$ Charging/discharging efficiency of ESS at bus j.

η_j^{loss} Fraction of stored energy lost per hour by ESS at bus j.

$\rho_j^{min}, \rho_j^{max}$ Minimum/maximum percentage magnitude of residual energy for ESS at bus j.

ρ_j^{ini} Initial percentage magnitude of residual energy for ESS at bus j.

t_k^{ϵ} Time duration consideration (interval number) for reserve category k of ESS.

$\mathcal{R}_{j,k}^{max}$ Maximum contribution of generator bus j for reserve category k.

RU_j, RD_j Ramp up/down rate limit of generator bus j.

t_j^{up}, t_j^{up} Minimum up/down time of generator bus j.

P_j^D, Q_j^D Real/reactive power demand at bus j.

r_{ij}, x_{ij} Line resistance/reactance of branch ij.

$\mathbf{D}_n$ The first-order difference matrix $\mathbf{D}_n \in \mathbb{R}^{n*(n+1)}$.

K_j^{st}, K_j^{sd} Start-up/shut-down operation cost at bus j.

K_j^{ε} Daily operation cost of ESS at bus j.

C. Variables

u_j^{ε} Binary variable for installing ESS at bus j.

$P_j^{\varepsilon,c}$ Active power production of ESS at bus j.

$P_j^{\varepsilon,d}$ Active power consumption of ESS at bus j.

$P_j^{\varepsilon}, Q_j^{\varepsilon}$ Active/reactive power production/consumption of ESS at bus j.

$E_j^{\varepsilon}(t)$ Residual capacity of ESS at bus j at time $t \in \mathcal{T}_0$.

Cap_j^{ε} Energy reservoir capacity of ESS at bus j.

$r_{j,k}^{\varepsilon}$ ESS reserve contribution for category k at bus j.

x_j Binary commitment state for unit j.

ϕ_j, ψ_j Binary startup/shutdown state for unit j.

P_j^G, Q_j^G Active/reactive power injection of bus j.

$r_{j,k}^G$ Reserve provision of bus j for category $k \in \Omega^r$.

P_{ij}, Q_{ij} Real/reactive power flow at the sending-end of line (i, j).

V_j, Λ_j Bus voltage magnitude at bus j and the square thereof: $\Lambda_j = |V_j|^2 = V_j V_j^*$.

I_{ij}, Γ_{ij} Current magnitude at the sending-end of line (i, j) and the square thereof.

D. Operators and Functions

$f_j(\bullet)$ Generation cost function of generator bus j.

$\bullet(t)$ Value of parameters or variables at time t.

$\bullet^{min}$ Minimum value of one variable.

$\bullet^{max}$ Maximum value of one variable.

1 Introduction

For ensuring the sustainability of electric power system, the share of renewable energy will continue to increase in the future. In distribution networks, however, the increasing penetration of wind and other forms of renewable energy sources (RES) as distributed generation (DG) presents significant challenges for maintaining the grid stability and reliability. ~~Being treated as *negative load*, the integration of wind power has been widely examined by considerable research. Without loss of generality, wind power is considered in this paper as the representative of intermittence and variability.~~ The intermittence and variability due to the integration of wind power is often represented as *negative load* and their impacts to the grid have been widely examined by considerable research. Research studies have indicated that ~~much more~~ excess reserve will be required in the presence of high wind power penetration [1] while wind turbines

themselves are incapable of providing the reserve service. As a result, replacing the fossil-fuel generators with non-dispatchable wind turbines would reduce the reserve provision which has to be compensated by either forcing fossil-fuel generators to operate further from their optimal set-points or resorting to alternative solutions such as energy storage systems (ESSs) [2].

ESS ~~provides~~ is a promising alternative helping utilities to facilitate the integration of wind power and improve the grid reliability and efficiency. ~~ESS is able to gain the~~ Direct benefit can be gained by buying and storing energy with a cheap price during off-peak periods and selling the stored energy back with a high price at peak times. This is termed as *arbitrage benefit* [3]. In addition, ESS can buffer the output of intermittent renewable sources. Within the context of a deregulated electricity market and an Active Distribution Network (ADN), as outlined in [2, 4], ESS shows much promise for mitigating the dynamics introduced by non-dispatchable variable generation [5], such as frequency regulation, deferring infrastructure upgrades, minimizing system losses, shaving peak load and so on [6]. However, the main disadvantage of ESS is its high installation and maintenance costs. This paper, therefore, examines the ESS placement in radial networks to provide reserve services and maximize the benefits of shareholders by taking full advantage of its arbitrage benefit. This can significantly help in wind variability regulating and total operation cost reduction with wind penetration. Besides providing reserve service, the energy pool of ESS is used to reduce generation cost, alleviate the line congestion, and ensure the voltage within specified range.

Regarding reserve support, there are many research studies devoted to market mechanisms to promote the development of ESS [7, 8]. These studies consider to make a profit out of the fluctuation of energy and reserve market prices. Other works for optimal operation of ESS have also given a glimpse of reserve provisioning [2, 9], such as [2] focused on ancillary services of ESS including reserve support. However, all these mentioned works mostly only concentrate on spinning reserve while the time duration limit of reserve support from ESS has not been considered. Herein, a much more comprehensive reserve provision is considered, including spinning reserve, upward and downward regulation reserves. In addition, the time duration constraint of ESSs' reserve provision has to be taken into account as the lasting reserve service cannot be provided with its limited energy capacity. Within this context, this paper aims to find the optimal planning and operation of ESS with widely adopting DG and RES in future microgrids, where localized distribution networks are disconnected from the traditional grid to operate autonomously. The reserve provisioning of ESS will help mitigate RES disturbances and network contingencies to strengthen grid resilience.

Research papers for the planning and operation of ESS can be divided into three categories: 1) ESS operation with unit commitment (UC) to provide reserve, shave peak load, minimize the total generation cost, and avoid extra start-up and shut-down operating cost [9–11]; 2) ESS planning and operation with optimal power flow (OPF) to alleviate the feeder flow capacity limitation and reduce line loss [12–14]; 3) combining ESS participation with UC and OPF together [4]. Although the third category could find the optimum, its formulation is difficult to solve in respect of the high computation complexity, especially with full AC-OPF consideration. Therefore, in [4], the ESS operation model

is simplified with reserve support ignored; whereas, in this paper, the problem is formulated with UC and AC-OPF integrated to find the optimal location and size for ESS installation in radial networks.

The AC-OPF model generally is non-convex and nondeterministic polynomial-time hard (NP-hard), and a large number of optimization algorithms and relaxations have been proposed. Blending UC and AC-OPF together makes the problem even more difficult to solve due to the binary variables and non-linear AC flow constraints. Thus, the *DistFlow* model for radial networks is adopted that motivated by the literature for the optimal placement and sizing of switched capacitors in distribution circuits for Volt/VAR control [15, 16]. A pioneering work of AC-OPF from Taylor [17] based on DistFlow equations derives a second-order cone programming (SOCP) model for distribution system reconfiguration, and is the first formulation with convex and continuous relaxations. Here, a mixed-integer SOCP (MISOCP) model with extended DistFlow equations is proposed to take advantage of both efficiency of DC-OPF and accuracy of full AC-OPF.

This paper adopts a deterministic programming model and converts the planning and operation of ESS into a finite time-series optimal control problem. The location and size allocation of ESSs among buses are coordinated with chronological commitment and dispatch model, and power flow model while respecting various operating reserve demand. The optimal solution is found as minimizing the operation cost of a multi-objective optimization problem with single day concerning. Although the total cost includes both the investment cost and the operation cost, only the operation cost is focused here as the investment cost has already been examined by other works (e.g. [4]) and is system dependent. The proposed model can be incorporated into long term models for deriving the overall cost as an aggregation analysis of multiple typical days. ~~Also, in the following isolated microgrid scenario, the reserve provision cost of the external grid is neglected, but it can be easily incorperated as additional objective terms.~~

The rest of this paper is organized as follows. Section 2 formulates the planning and operation of ESS as a MISOCP model ~~explored in this paper~~. Simulated case studies are illustrated in Section 3 with reference to realistic data and a standard test-feeder network topology. Conclusions are drawn in Section 4.

2 Problem Formulation

ESS is able to play the role of generator and consumer at the same time, and improve the stability and reliability of system by providing reserve services. However, its economic feasibility should be justified ~~as ESSs are expensive~~ for its high installation and maintenance costs. There are many factors contributed to the recovery of ESS investment cost: 1) income from price arbitrage; 2) earning from the reserve cost ~~for high wind penetration, plus provisioning of reserve could reduce the number of dispatching operation and avoid ESS wear~~; 3) reduction of start-up and shut-down operation cost of fossil generator; 4) reduction of transmission line loss ~~due to the dispersal of loss over the network~~. ~~Engaging in reserve markets alone would not be enough to recover the full capital costs of ESS.~~ Its participation in

various lucrative situations is critical to enlarge the expected income. This paper formulates the model to fully and effectively use the limited energy reservoir capacity to maximize the revenue of shareholders and exert the arbitrage benefit of ESS as much as possible. Besides reserve support, ESS is used to reduce generation cost, alleviate line congestion, and ensure voltages within specified range, etc.

Connected graph (more specifically a tree) $\mathcal{G} = (\mathcal{N}, \mathcal{L})$ is used to represent a power radial network, where each node j in $\mathcal{N}$ denotes a bus and each link (i, j) in $\mathcal{L}$ denotes a line. In each time duration, generation/consumption variables of generators, renewable resources and ESSs are considered as constant. Herein the planning and operation of ESS are formulated in radial networks and integrated with UC and OPF to find the optimal location and size for storage unit installation.

2.1 Reserve Demand

~~With the increase of wind penetration in power supply, more conventional generators are replaced with non-dispatchable wind turbines which are incapable of providing reserve support [2].~~ High wind penetration would ~~therefore~~ not only increase the reserve cost but also deteriorate the reserve support sources. ~~Furthermore,~~ The fluctuation of wind power would also increase reserve requirements. In order to hedge deviation of wind power, sufficient reserve has to be maintained in the system. The deployment of ESS can be resorted as an alternative solution, and its fast-response ability would enable it to participate in various reserve provisioning.

In this paper, the reserve provision consists of three kinds of operating reserve services, namely: spinning reserve, upward and downward regulation reserves (set Ω^r). The reserve requirements ($\mathcal{R}_k$), which can be specified by the system operator (SO), are assumed to be constant during the scheduling period. In considering the wind variability and uncertainty, an extra reserve demand, termed as *wind disturbance reserve* and denoted as $\mathcal{R}_\delta$, is added to above reserve categories to accommodate the wind power deviation. Let P_w be the forecast wind power and $\tilde{P}_w$ be the actual output, the prediction error $\delta p(t)$ is

$$\delta p(t) = P_w(t) - \tilde{P}_w(t) \tag{1}$$

and wind disturbance reserve is defined as the maximum absolute prediction error, i.e. $\mathcal{R}_\delta = max(|\delta p(t)|)$.

Spinning reserve is defined as the unused capacity of connected and synchronized generation, which can be instantaneously utilized in response to a disturbance or activated by the SO [18]. Unplanned outages of generation units and wind power deviation due to forecasting error can result in unpredictable imbalances between generation and load, which need to be compensated by the spinning reserve. Thus here, wind disturbance reserve $\mathcal{R}_\delta$ is added to the spinning reserve demand $\mathcal{R}_{sp}$, and ESS is considered as on-line generators to undertake this task with fossil generators.

Regulation reserve provided by units under direct real-time control of SO is used to fine-tune the frequency of the grid by matching supply with demand [19]. There are two types of regulation reserve: upward and downward. Upward

regulation reserve is the sum of increasable margin between the current output and the maximum loading limit of all units. Downward regulation reserve, in comparison, is the buffer demand for current outputs being higher than the minimum output limits. Since wind deviation could be positive or negative, both types of regulation reserves should take the wind disturbance reserve into account. ESS is particularly suitable for providing regulation reserves through charging and discharging.

2.2 ESS Planning and Operation

While ESSs will not be collocated with wind turbines or fossil generators in this paper, there can be different placement modes for ESS in a radial network. On the one hand, ESS can be placed near the root node (substation bus) to stabilize variable power production and maximize the transmission line capacities. On the other hand, installing ESS on the leaf node can improve the voltage of remote nodes and alleviate the local line congestion. With a restricted budget, the location and size of ESS should consider factors such as land availability and spot price profile, and be collaborated with the operation of ESS to find the optimal solution with minimum cost. It is assumed that both dispatchable fossil generators and ESS have the capability of supporting the network with both active and reactive power, and the production/consumption of reactive power from a ESS does not affect its energy reservoir level.

$$\sum\nolimits_{j\in\mathcal{N}} u_j^{\varepsilon} \le U^{\varepsilon} \tag{2}$$

$$\sum\nolimits_{j\in\mathcal{N}} Cap_j^{\varepsilon} \le Cap_{sum}^{\varepsilon} \tag{3}$$

$$u_j^{\varepsilon} Cap_j^{\varepsilon,min} \le Cap_j^{\varepsilon} \le u_j^{\varepsilon} Cap_j^{\varepsilon,max} \tag{4}$$

$$P_j^{\varepsilon}(t) = P_j^{\varepsilon,c}(t) + P_j^{\varepsilon,d}(t), \quad -P_j^{\varepsilon,max_c} \le P_j^{\varepsilon,c}(t) \le 0, \quad 0 \le P_j^{\varepsilon,d}(t) \le P_j^{\varepsilon,max_d} \tag{5}$$

$$-u_j^{\varepsilon} P_j^{\varepsilon,max_c} \le P_j^{\varepsilon}(t) \le u_j^{\varepsilon} P_j^{\varepsilon,max_d} \tag{6}$$

$$-u_j^{\varepsilon} Q_j^{\varepsilon,max} \le Q_j^{\varepsilon}(t) \le u_j^{\varepsilon} Q_j^{\varepsilon,max} \tag{7}$$

$$P_j^{\varepsilon}(t)^2 + Q_j^{\varepsilon}(t)^2 \le (S_j^{\varepsilon,max})^2 \tag{8}$$

$$\Delta E_j^{\varepsilon}(t) = -\Delta t[\eta_j^{in} P_j^{\varepsilon,c}(t) + 1/\eta_j^{out} \cdot P_j^{\varepsilon,d}(t)] \tag{9}$$

$$E_j^{\varepsilon}(t) = E_j^{\varepsilon}(t-1) + \Delta E_j^{\varepsilon}(t) - \Delta t \frac{\eta_j^{loss}}{2} [E_j^{\varepsilon}(t) + E_j^{\varepsilon}(t-1)] \tag{10}$$

$$E_j^{\varepsilon}(0) = Cap_j^{\varepsilon} \cdot \rho_j^{ini} \tag{11}$$

$$Cap_j^{\varepsilon} \cdot \rho_j^{min} \le E_j^{\varepsilon}(t) \le Cap_j^{\varepsilon} \cdot \rho_j^{max} \tag{12}$$

Inequalities (2) and (3) are the quota on the number and the restriction on the maximum of total energy reservoir capacity imposed upon ESS placement in the whole network. ~~Based on the assumption that ESSs are interfaced with the grid using a power electronic converter,~~ Constraint (4) further bounds ESSs' ~~installation~~ capacity for a particular bus j. As for dispatching, the active power of charging/discharging (consumption/production) has the constraints: (5) and (6), and the reactive power is confined by (7). The charging and discharging operations are mutually exclusive, thus only one variable of $P_j^{\varepsilon,c}(t)$ and $P_j^{\varepsilon,d}(t)$ is non-zero in (5). Equation (8) models the capability curve of active and reactive power. With time t, (9) denotes the capacity changes due to dispatching operation of ESS. Considering self-discharging loss with the coefficient η_j^{loss}, there is the equality (10) describing the capacity relationship between time $t-1$ and t. Equation (11) defines the initial energy capacity of ESS, and (12) maintains its capacity within the safety range (for prolonging the life cycle) .

2.3 ESS Reserve Provisioning

As mentioned, ESS can provide ~~various~~ three kinds of operating reserve services ~~. Normally, the spinning and upward regulation reserves of one generator are different owing to distinct response time and time duration requirements. But here, the spinning reserve provision of ESS is set equal to the value of upward regulation reserve~~ in view of its quick response capability. Both spinning and upward regulation reserves are related to discharging operations of ESS for providing the extra output buffer, thus a subset of reserve category $\Omega^{r\prime} = \{sp, up\} \subset \Omega^r$ is defined to express their constraints jointly. With reserve provisioning, the magnitude of reserve plus actual dispatching power should be less than the maximum charging/discharging power:

$$r_{j,k}^{\varepsilon}(t) + P_j^{\varepsilon}(t) \leq u_j^{\varepsilon} P_j^{\varepsilon,max_d}, \quad \forall k \in \Omega^{r\prime} \tag{13}$$

$$r_{j,dw}^{\varepsilon}(t) - P_j^{\varepsilon}(t) \leq u_j^{\varepsilon} P_j^{\varepsilon,max_c} \tag{14}$$

Unlike generator being able to provide lasting reserve support, the limited reservoir capacity of ESS results in that its reserve provision is time-limited. Hence, the ~~time duration~~ capacity constraints ~~of various operating reserves~~ are added as follows:

$$E_j^{\varepsilon}(t) - \Delta t/\eta_j^{out} \cdot [r_{j,k}^{\varepsilon}(t) + P_j^{\varepsilon}(t)] \geq Cap_j^{\varepsilon} \cdot \rho_j^{min}, \quad \forall k \in \Omega^{r\prime} \tag{15}$$

$$E_j^{\varepsilon}(t) + \Delta t \cdot \eta_j^{in} \cdot [r_{j,dw}^{\varepsilon}(t) - P_j^{\varepsilon}(t)] \leq Cap_j^{\varepsilon} \cdot \rho_j^{max} \tag{16}$$

The reserve capacity is used for emergency situations, and the required time duration is also needed to be considered. If the time duration is set to t_k^{ϵ} (the number of time intervals), then the following constraints must be met:

$$E_j^{\varepsilon}(t) - \frac{\Delta t}{\eta_j^{out}} \sum_{\tau=t}^{\hat{\tau}} r_{j,k}^{\varepsilon}(\tau) \geq Cap_j^{\varepsilon} \cdot \rho_j^{min}, \quad \hat{\tau} = min(t + t_k^{\epsilon}, T), \quad \forall k \in \Omega^{r'} \tag{17}$$

$$E_j^{\varepsilon}(t) + \Delta t \cdot \eta_j^{in} \cdot \sum_{\tau=t}^{\hat{\tau}} r_{j,dw}^{\varepsilon}(\tau) \leq Cap_j^{\varepsilon} \cdot \rho_j^{max}, \quad \hat{\tau} = min(t + t_{dw}^{\epsilon}, T) \tag{18}$$

2.4 Unit Commitment

The load demand is supplied by dispatchable fossil units and wind turbines. As a kind of energy pool, ESS can perform the peak shaving and valley filling of load. In the context of UC, the dispatching operations of ESS avoid excessive start-up and shut-down actions of fossil generators and reduce total generation cost. ~~For expressing the constraint, the first-order difference matrix is introduced and denoted as $\mathbf{D}_n \in \mathbb{R}^{n*(n+1)}$. Here, $\mathbf{D}_T \in \mathbb{R}^{T*(T+1)}$ and $\mathbf{D}_{(T-1)} \in \mathbb{R}^{(T-1)*T}$ will be used.~~ Unless otherwise stated, the following constraints are considered with subscript: $j \in \mathcal{N}^g, t \in \mathcal{T}$. For generator j, the minimum up and down time limits are:

$$x_j(t) - x_j(t-1) \geq x_j^{\tau}, \quad \forall \tau \in [t+1, min\{t + t_j^{up} - 1, T\}], t \in [2, T] \tag{19}$$

$$x_j(t) - x_j(t-1) \leq 1 - x_j^{\tau}, \quad \forall \tau \in [t+1, min\{t + t_j^{dw} - 1, T\}], t \in [2, T] \tag{20}$$

The ramp up and down rate limits are:

$$-RD_j \cdot \mathbf{1}_{(T-1)} \leq \mathbf{D}_{(T-1)} P_j^G \leq RU_j \cdot \mathbf{1}_{(T-1)} \tag{21}$$

where $\mathbf{1}_{(T-1)} \in \mathbb{R}^{T-1}$ is a vector with all elements as 1. Range regarding reactive power output is:

$$Q_j^{G,min} x_j(t) \leq Q_j^G(t) \leq Q_j^{G,max} x_j(t) \tag{22}$$

In light of active power output $P_j^G(t)$, various reserves should meet the following constraints:

$$P_j^G(t) + r_{j,sp}^G(t) \leq P_j^{G,max} x_j(t), \quad r_{j,sp}^G(t) \geq 0 \tag{23}$$

$$P_j^G(t) + r_{j,up}^G(t) \le P_j^{G,max} x_j(t), \quad r_{j,up}^G(t) \ge 0 \tag{24}$$

$$P_j^{G,min} x_j(t) \le P_j^G(t) - r_{j,dw}^G(t), \quad r_{j,dw}^G(t) \ge 0 \tag{25}$$

The reserve contribution of each generator is restricted:

$$r_{j,k}^G(t) \le \mathcal{R}_{j,k}^{max} x_j(t), \quad k \in \Omega^r \tag{26}$$

where $\mathcal{R}_{j,k}^{max}$ is the maximum contribution of generator j for reserve category k. The unit on/off, startup and shutdown indicators are linked by the following relations:

$$\mathbf{D}_T * x_j = \phi_j, -\mathbf{D}_T * x_j = \psi_j, \quad \forall j \in \mathcal{N}^g \tag{27}$$

Finally, the reserve sum of generators and ESSs should satisfy each kind of demand:

$$\sum\nolimits_{j \in \mathcal{N}^g} r_{j,k}^G(t) + \sum\nolimits_{j \in \mathcal{N}} r_{j,k}^{\mathcal{E}}(t) \ge \mathcal{R}_k, \quad \forall k \in \Omega^r, t \in \mathcal{T} \tag{28}$$

2.5 Radial AC-OPF

Considering the ESS placement in radial distribution networks, the network security constraints adopt the SOCP formulation for the radial AC network proposed in [17]. If not otherwise stated, the rest of this section is considered with subscript: $j \in \mathcal{N}, (i,j) \in \mathcal{L}, t \in \mathcal{T}$. The square of nodal voltage magnitude and feeder current flow are defined as:

$$\Lambda_j(t) = V_j(t)^2 \tag{29}$$

$$\Gamma_{ij}(t) = I_{ij}(t)^2 = \frac{P_{ij}(t)^2 + Q_{ij}(t)^2}{\Lambda_i(t)} \tag{30}$$

Variables $V_j(t)$ and $I_{ij}(t)$ are not used in the following formulation, and therefore can be omitted hereinafter.

$$P_{ij}(t) - r_{ij}\Gamma_{ij}(t) - \sum_{k:(j,k)\in\mathcal{L}} P_{jk}(t) = P_j^D(t) - P_j^G(t) - P_j^{\mathcal{E}}(t) \tag{31}$$

$$Q_{ij}(t) - x_{ij}\Gamma_{ij}(t) - \sum_{k:(j,k)\in\mathcal{L}} Q_{jk}(t) = Q_j^D(t) - Q_j^G(t) - Q_j^{\mathcal{E}}(t) \tag{32}$$

$$\Lambda_j(t) = \Lambda_i(t) - 2[r_{ij}P_{ij}(t) + x_{ij}Q_{ij}(t)] + (r_{ij}^2 + x_{ij}^2)\Gamma_{ij}(t) \tag{33}$$

$$\Gamma_{ij}(t) \le \Gamma_{ij}^{max} \tag{34}$$

$$\Lambda_j^{min} = (V_j^{min})^2 \le \Lambda_j(t) \le \Lambda_j^{max} = (V_j^{max})^2 \tag{35}$$

For the bus j at time t, constraints (31) and (32) respectively account for the balance of active and reactive power flows with branch flow variables at the sending-end of lines: the incoming active/reactive power flow of bus j (from bus i to bus j) minus the line loss and the flow sum of leaving lines that is equal to the net injection on the bus j. The nodal voltages of bus i and j along the feeder (i, j) have the constraint (33). The square of line current is within the range $(0, \Gamma_{ij}^{max}]$ by (34), and the voltage at bus j is restricted within $[V_j^{min}, V_j^{max}]$ by (35). Without sacrificing accuracy, equation (30) can be relaxed in the form of a rotated quadratic cone of SOCP format:

$$\left\| \begin{array}{c} 2P_{ij}(t) \\ 2Q_{ij}(t) \\ \Gamma_{ij}(t) - \Lambda_i(t) \end{array} \right\|_2 \le \Gamma_{ij}(t) + \Lambda_i(t) \tag{36}$$

2.6 Composite Objective

This paper only considers the operation cost based on single day concerns, and is devoted to provide an efficient planning and operation model in an isolated microgrid scenario which can be embedded into related research for long term planning (e.g. [4]). It neglects the reserve provision cost of the external grid, and investment costs involving ESS installation and maintenance. In view of charging and discharging operations of ESS, its engagement in the grid can alleviate the feeder congestion, reduce the line loss and ensure the voltage magnitude within the specified range. Aiming at reducing the running cost of system, the location and size selection of ESS is crucial important.

Indexed by time t, the aggregation generation cost of all units is defined as:

$$C^G(t) = \sum\nolimits_{j \in \mathcal{N}^g} f_j\left(P_j^G(t)\right) \tag{37}$$

The cost of unit start-up and shut-down operations is:

$$C^S(t) = \sum\nolimits_{j \in \mathcal{N}^g} \phi_j(t) K_j^{st} + \psi_j(t) K_j^{sd} \tag{38}$$

After omitting the self-discharge loss, the dispatching loss of ESS is:

$$\Theta_\ell^\varepsilon(t) = (1 - \eta_j^{in}) P_j^{\varepsilon,c}(t) + (1/\eta_j^{out} - 1) P_j^{\varepsilon,d}(t) \tag{39}$$

The daily operation cost of all installed ESS is:

$$C^\varepsilon = \sum\nolimits_{j \in \mathcal{N}} u_j^\varepsilon K_j^\varepsilon \tag{40}$$

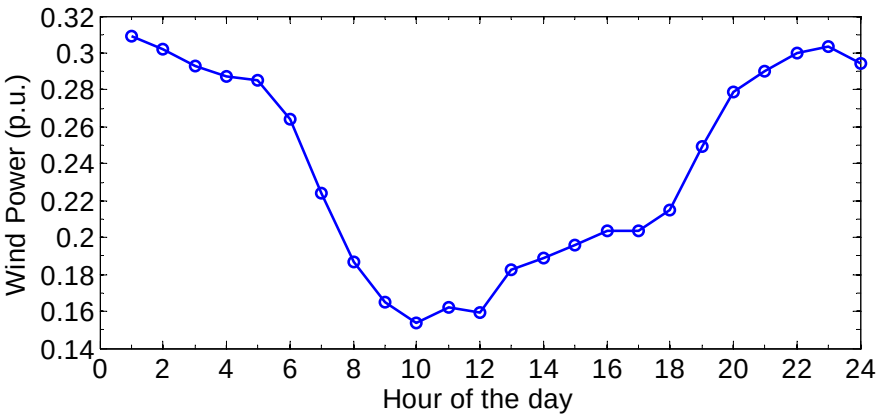

Fig. 1 *Average daily wind power curve.*

Taken together, the daily objective cost is as follows:

$$\begin{cases} \min\limits_{\boldsymbol{\Xi},\mathbf{X}} & \sum\limits_{t=1}^{T}\left[W_g C^G(t)+W_s C^S(t)+W_\ell^\varepsilon \Theta_\ell^\varepsilon(t)\right]+W_\varepsilon C^\varepsilon \\ \text{s.t.} & \text{ESS planning and operation: } eqs.\ (2)-(12) \\ & \text{ESS reserve provioning: } eqs.\ (13)-(18) \\ & \text{UC: } eqs.\ (19)-(28) \\ & \text{OPF: } eqs.\ (31)-(36) \end{cases} \tag{41}$$

where $\boldsymbol{\Xi}=\{u_j^\varepsilon, Cap_j^\varepsilon, P_j^{\varepsilon,c}, P_j^{\varepsilon,d}, Q_j^\varepsilon, r_{j,k}^\varepsilon, x_j, P_j^G, Q_j^G, r_{j,k}^G\}$ is the set of decision variables, and $\mathbf{X}=\{E_j^\varepsilon, \phi_j, \psi_j, \Lambda_j, \Gamma_{ij}, P_{ij}, Q_{ij}\}$ is the state variable set. W_g, W_s, W_ℓ^ε, and W_ε are the weighting coefficients for generation cost, unit start-up/shut-down cost, round trip efficiency loss and daily operation cost of ESS, which are determined by using the analytic hierarchy process (AHP) [20].

3 Simulations

In this section, the effects of ESS are illustrated using IEEE benchmark radial distribution systems with wind energy penetration. Due to space limitation, only the results from the IEEE 34-bus test system are reported here. Considering the relative proximity of network, it is assumed that the wind speed across all buses (wind turbine sites) is the same and the probability density function (PDF) for wind speed follows the Rayleigh distribution. Rayleigh PDF is one of probabilistic expressions widely used to model the behaviour of wind. It is a special form of Weibull PDF with shape factor $k=2$ [21, 22]. The sample data of wind speed, measured by Blue Hill Observatory [23] and within range $[0,27]$, are converted into the wind power by adopting Rayleigh PDF and the linear approximation of speed-power relation curve as in [22]. All parameters used can be found in [22], and the daily average wind power curve is depicted in Fig.

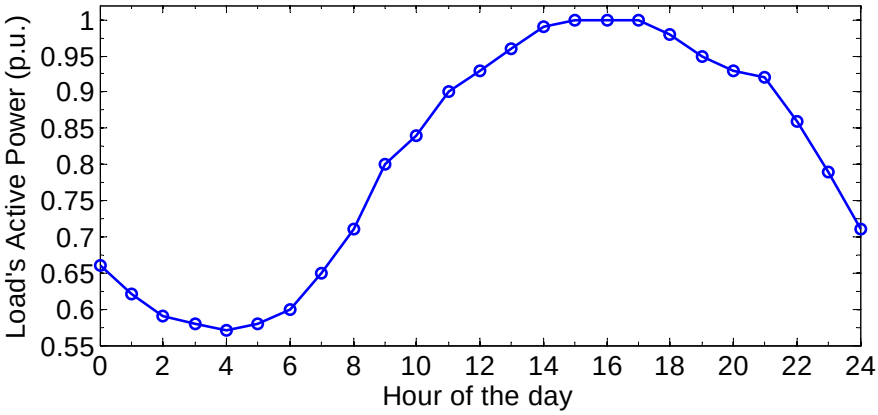

Fig. 2 *CAISO's summer daily load curve.*

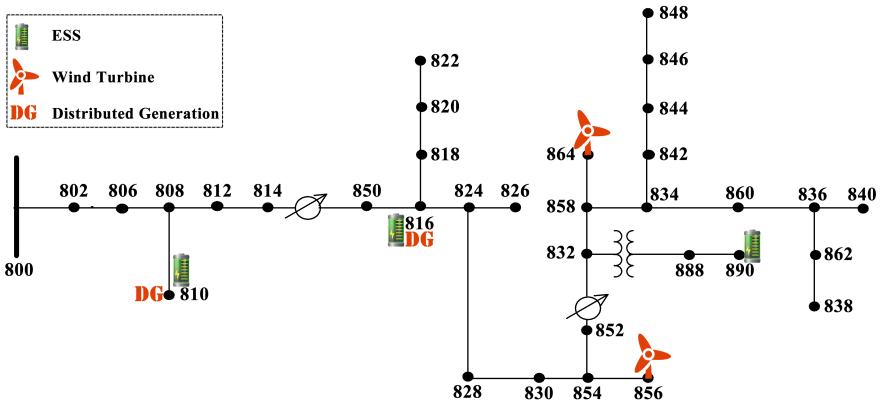

Fig. 3 *IEEE 34-bus test feeder.*

1 with rated power of 1 p.u. The wind penetration level, L_w, is define as the ratio of the total peak wind power to the rated output sum of all fossil generators. With specified wind penetration level, the peak wind value is fixed and the daily wind output profile follows the curve in Fig. 1.

A typical summer load curve of 2006 for the California Independent System Operator (CAISO) [24] is shown in Fig. 2, which comprises three load levels or periods in a day: peak, intermediate, and off-peak. The amplitude of load profile is normalized with peak demand of 1 p.u. In following cases, only the peak load is specified, denoted as $P^{D,max} = max(P^D(t)) : t \in \mathcal{T}$, and the remain daily load profile follows the curve in Fig. 2 proportionally.

As for the radial network, the modified IEEE 34-bus distribution test feeder [25] is used as shown in Fig. 3. It is supposed to have two dispatchable fossil generators at bus 810 and 816, and two non-dispatchable wind farms connected at bus 856 and 864, respectively. All fossil generators and wind farms are assumed to have same parameters respectively. Wind energy is set to be free for brevity. All parameters are listed in Table 1. The output of wind power is specified within study cases for various penetration levels. ~~Both fossil generators are with minimum output 0.2 p.u. and rated output 0.5 p.u, and their total rated output is 1.0 p.u.~~ According to the wind penetration level definition, levels 10%, 15% and 20% correspond to peak wind power of 0.10, 0.15 and 0.20 (p.u.) respectively. The wind disturbance

Table 1 Simulation Parameters

Base Power	1 MW	Base Voltage	1.06 kV
U^{ε}	5	Cap^{ε}_{sum}	1.0 MWh
P^{ε,max_c}	0.03 p.u.	P^{ε,max_d}	0.03 p.u.
$Cap^{\varepsilon,min}$	0.2 MWh	$Cap^{\varepsilon,max}$	0.3 MWh
ρ^{min}	0.25	ρ^{max}	0.95
ρ^{ini}	0.25	η^{loss}	0.05
η^{in}	0.90	η^{out}	0.90
$P^{G,min}$	0.2 p.u.	$P^{G,max}$	0.5 p.u.
$Q^{G,min}$	−1.5 p.u.	$Q^{G,max}$	1.5 p.u.
t^{up}	3 hr	t^{dw}	2 hr
K^{st}	50 $	K^{sd}	10 $
K^{ε}	500 $	Δt	1 hr
Quadratic cost function $f(x) = ax^2 + bx + c$, $a = 0.203(\$/MW^2)$, $b = 7.629(\$/MW)$, $c = 217.4(\$/hr)$			

reserve $\mathcal{R}_{\delta}$ is set to 25% of peak value of wind output. For operating reserve requirement setting, spinning reserve is: $\mathcal{R}_{sp} = 0.35 + \mathcal{R}_{\delta}$, and upward and downward regulation reserves both are equal to $P^{D,max} * 0.15 + \mathcal{R}_{\delta}$. ~~The total energy capacity of ESS (Cap^{ε}_{sum}) is 1 p.u., and the maximum installation number is 5.~~ The candidates locations of ESS are either near the substation nodes or near leaf nodes, and set to the node collection {808, 810, 816, 820, 822, 838, 840, 848, 850, 856, 864, 888,890}. The cost weighting coefficients W_g, W_s, W^{ε}_{ℓ}, and W_{ε} are set to 0.015, 0.015, 0.32 and 0.65, respectively.

It is expected that the reserve provisioning stress can be relieved with ESS participation. In order to quantify the reserve support of ESS, the following scenario is considered: the peak load is set to 0.9 p.u. and the wind penetration level is 15% (0.15 p.u.). Through solving the proposed model, three ESSs are put at bus 810, 816 and 850. The ~~resulting~~ reserve curves of maximum daily output and requirement are depicted in Fig. 4 with respect to all three kinds of operating reserve. The horizontal lines represent the reserve demand, and the maximum output ("Max Res.") and requirement ("Req. Res.") of one kind of reserve are marked with the same color. Fig. 4a shows that without ESS participation downward regulation reserve is insufficient and the reliable running of grid is infeasible. However, along with ESS as in Fig. 4b and 4c, more reserve space is supplemented and the reserve requirement hence is satisfied. In addition, it is observed that the amplitude of operating reserves provided by ESS with time duration consideration in Fig. 4c is less than that without time duration limitation as shown in Fig. 4b. The reason is that ESSs' limited capacity cannot guarantee the lasting reserve support. Hence, with ESS participating in reserve provision, the time duration of reserve must be taken into account to get the precise result.

High wind penetration will increase the reserve requirements and influence the cost and operation of the grid. To illustrate the effect of wind penetration, a group of cases with three load scales (with daily peak values of 0.6 p.u.,

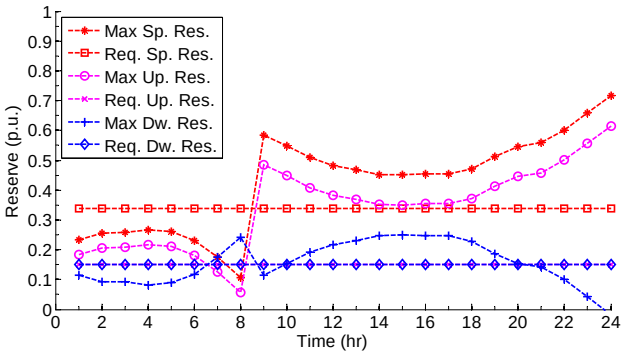

(a) Only fossil generators support.

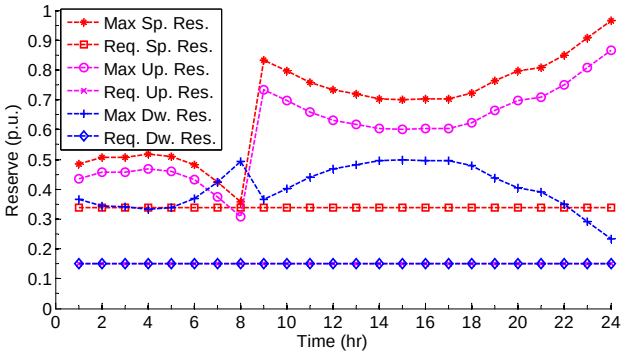

(b) Without time duration restriction after ESS participation.

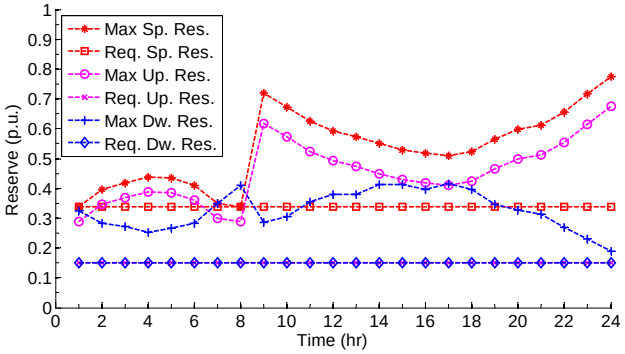

(c) With time duration restriction after ESS participation.

Fig. 4 *Profiles of operating reserve with various provisioning scenarios.*

0.9 p.u., and 1.08 p.u.) and three wind penetration levels (10%, 15% and 20%) are considered. Combined together, nine cases are tested for comparison. ~~It should be pointed out that r^{ε}_{op} is equivalent to r^{ε}_{up} as mentioned in Section 2.3, thus r^{ε}_{op} is omitted in the table.~~ As can be seen from Table 2, the per unit cost of load is reduced as wind penetration level and load scale increasing, which means that larger load can absorb the variability of wind power more easily. In each group of cases with fixed load profile, more wind disturbance reserve support is required and the objective cost is reduced with higher wind energy penetration. For the ESS placement, the results of the second and third groups are exactly the opposite. In the former group more number of ESS are placed in the network as the wind penetration level increases, but for latter group the number is decreased. It can be observed that ESSs tend to use their available reservoir

Table 2 Cases with various wind penetration levels and load scales

Group	$P^{D,max}$ $p.u.$	L_w %	ESS num.	$Cap.$ MWh	ESS buses	$\mathcal{R}_\delta$ $p.u.$	$\Theta^{\varepsilon}_{\ell}$ $p.u.$	C^S \$	C^G 10^3\$	ΔC^G \$/MWh	C^{obj} 10^3\$	ΔC ⋆ \$/MWh
1	0.60	10	5	1.0	816, 820, 850, 864, 888	0.0377	0.1004	60	7.2425	814.8	9.8035	1012.7
		15	5	1.0	810, 820, 816, 850, 888	0.0502	0.1119	60	7.0197	858.1	9.5808	989.7
		20	5	1.0	808, 820, 816, 850, 888	0.0752	0.1342	60	6.8014	843.5	9.3627	967.1
2	0.90	10	2	0.4	810, 888	0.0377	0.0409	0	10.5453	736.7	11.5457	795.1
		15	4	0.8	810, 816, 820, 888	0.0502	0.0705	60	9.4472	734.2	11.5079	792.5
		20	5	1.0	810, 816, 820, 850, 888	0.0752	0.0809	60	8.7877	737.6	11.3485	781.5
3	1.08	10	4	0.8	806, 810, 820, 888	0.0377	0.0436	0	10.5635	634.4	12.5639	721.0
		15	3	0.6	806, 810, 888	0.0502	0.0396	0	10.5594	654.7	12.0598	692.1
		20	2	0.6	806, 810	0.0752	0.1281	0	10.5619	641.9	11.5632	663.6

⋆ $P^{D,max}$: daily peak load; L_w: wind penetration level; $Cap.$: ESS capacity sum; $\mathcal{R}_\delta$: wind disturbance reserve; $\Theta^{\varepsilon}_{\ell}$: round-trip efficiency loss of ESS; C^S: unit start-up/shut-down cost; C^G: generation cost; ΔC^G: per unit generation cost; C^{obj}: objective cost; ΔC: per unit cost of load.

to provide reserve support in the second group, where the lower load results in one unit switches off and the reserve provision depends on increasing number of ESS. In the third group, the peak demand approaches the generation supply limit, ESSs are used to store energy during off peak periods and discharge power at peak times. For this reason, in this group the lower wind penetration level requires more number of ESS. ~~From the first and second group data of results, we can observe that the generation and operation cost may not be reduced as penetration level increasing, which is resulted from the extra start-up of generator for reserve support. The third group data shows that the generation cost is reduced as penetration level increasing but the total operation cost with $L_w = 20$ is increased compared to that with $L_w = 15$. Although wind power can be delivered to part of load which reduces fuel consumption, more wind disturbance reserve demand requires frequent dispatching operations of ESS, thus, increasing the operation cost. The desirable outcome with both decreased generation cost and operation cost is obtained in the final group.~~ All these cases are infeasible without ESS owing to insufficient reserve provision. The participation of ESS is indispensable for incorporating wind energy to hedge against uncertainty.

The YALMIP, a Matlab toolbox for modelling and optimization [26], is used to implement the proposed formulation. Since the formulation is a MISOCP problem, the branch-and-bound algorithm is employed to find the optimal solution by using the Gurobi solver [27] and running on 3.3 GHz Intel Core i3-3220 computer with 4 GB of RAM. For the above cases based on IEEE 34-bus distribution network, the solver needs to cope with nearly 14,860 variables and 8,900 constraints. The mixed numerous binary variables make the problem solving intractable, and the average computation time is about five minutes. Although the proposed MISOCP model can be handled within mentioned setting environment, the mixed-integer SOCP has not attained the same maturity as mixed-integer linear or quadratic programming (QP), which makes the proposed model infeasible for larger instances. The slightly increase of unit number or ESS quota number, even more considering in a bigger network with more nodes, will make the computation complexity grow at an exponential rate. However, cutting planes and improved continuous relaxation procedures

are active areas of research [17], and substantial efficiency improvements are expected in the near future.

4 Conclusion

To incorporate the RES such as wind power and solar generators, the present and future power network demands extra flexibility more than ever. In this paper, ESS is used to provide reserve services including spinning reserve, upward and downward regulation reserves for wind penetration. Considering the variability and uncertainty of non-dispatchable wind power, specialized wind disturbance reserve has been provided. Since the energy reservoir capacity of ESS is limited and cannot provide lasting reserve support, the time duration of reserve support has been taken into account. With various wind penetration levels and load scales, study cases referring to the radial topology of IEEE 34-bus distribution test feeder were used to demonstrate the effectiveness and capability of the proposed methodology. It has been shown that the proposed MISOCP formulation is effective and efficient for ESS planning and operation using convexifying integrated UC and AC-OPF models. Simulation results testified that the reserve provision would be insufficient and the grid cannot operate reliably without ESS participation, and more accurate solution could be derived by considering the time duration of ESSs' reserve support. It is possible to conclude that ESS has enormous potential to reduce the operation cost of system in presence of high wind power penetration in the future.

5 Acknowledgement

The authors gratefully acknowledge the support of the Hong Kong Polytechnic University under Project G-UA3Z. Mr. Qin, Mr. Luo, and Miss Wu would also like to acknowledge their PhD Research Studentship awarded by the University.

6 References

[1] Halamay D. A., Brekken T. K., Simmons A., and McArthur S.: 'Reserve requirement impacts of large-scale integration of wind, solar, and ocean wave power generation', *IEEE Trans. Sustain. Energy*, 2011, **2**, (3), pp. 321–328

[2] Abdelouadoud S. Y., Girard R., and Guiot T.: 'Planning-oriented yearly simulation of energy storage operation in distribution system for profit maximization, voltage regulation and reserve provisionning'. Proc. *IET 22nd CIRED*, 2013, pp. 1–4

[3] Awad A. S. A., EL-Fouly T. H. M., and Salama M. M. A.: 'Optimal ESS Allocation for Load Management Application', *IEEE Trans. Power Syst.*, 2015, **30**, (1), pp. 327–336

[4] Nick M., Cherkaoui R., and Paolone M.: 'Optimal Allocation of Dispersed Energy Storage Systems in Active Distribution Networks for Energy Balance and Grid Support', *IEEE Trans. Power Syst.*, 2014, **29**, (5), pp. 2300–2310

[5] Usama M. U., Kelle D., and Baldwin T.: 'Utilizing spinning reserves as energy storage for renewable energy integration'. Proc. *Proc. IEEE PSC*, Clemson University, 2014, pp. 1–5

[6] Eyer J. and Corey G.: 'Energy storage for the electricity grid: Benefits and market potential assessment guide', *Sandia National Laboratories*, 2010

[7] Akhavan-Hejazi H. and Mohsenian-Rad H.: 'Optimal operation of independent storage systems in energy and reserve markets with high wind penetration', *IEEE Trans. Smart Grid*, 2014, **5**, (2), pp. 1088–1097

[8] Ding H., Hu Z., and Song Y.: 'Rolling Optimization of Wind Farm and Energy Storage System in Electricity Markets', *IEEE Trans. Power Syst.*, 2015, **30**, (5), pp. 2676–2684

[9] Hu Z., Zhang S., Zhang F., and Lu H.: 'SCUC with battery energy storage system for peak-load shaving and reserve support'. Proc. *Proc. IEEE PES Gen. Meet.* 2013, pp. 1–5

[10] Daneshi H and Srivastava A.: 'Security-constrained unit commitment with wind generation and compressed air energy storage', *IET Gener. Transm. Distrib.*, 2012, **6**, (2), pp. 167–175

[11] Pozo D., Contreras J., and Sauma E. E.: 'Unit Commitment With Ideal and Generic Energy Storage Units', *IEEE Trans. Power Syst.*, 2014, **29**, (6), pp. 2974–2984

[12] Gayme D. and Topcu U.: 'Optimal power flow with large-scale storage integration', *IEEE Trans. Power Syst.*, 2013, **28**, (2), pp. 709–717

[13] Nick M., Hohmann M., Cherkaoui R., and Paolone M.: 'Optimal location and sizing of distributed storage systems in active distribution networks'. Proc. *Proc. IEEE PowerTech*, Grenoble, France, 2013, pp. 1–6

[14] Jabr R. A., Dzafic I., and Pal B. C.: 'Robust Optimization of Storage Investment on Transmission Networks', *IEEE Trans. Power Syst.*, 2015, **30**, (1), pp. 531–539

[15] Baran M. E. and Wu F. F.: 'Optimal capacitor placement on radial distribution systems', *IEEE Trans. Power Del.*, 1989, **4**, (1), pp. 725–734

[16] Baran M. E. and Wu F. F.: 'Optimal sizing of capacitors placed on a radial distribution system', *IEEE Trans. Power Del.*, 1989, **4**, (1), pp. 735–743

[17] Taylor J. A. and Hover F. S.: 'Convex models of distribution system reconfiguration', *IEEE Trans. Power Syst.*, 2012, **27**, (3), pp. 1407–1413

[18] Rebours Y. and Kirschen D.: 'What is spinning reserve', *The University of Manchester*, 2005, pp. 1–11

[19] Bessa R. J. and Matos M. A.: 'Economic and technical management of an aggregation agent for electric vehicles: a literature survey', *Euro. Trans. Electr. Power*, 2012, **22**, (3), pp. 334–350

[20] Saaty T. L.: 'Decision making-the analytic hierarchy and network processes (AHP/ANP)', *J. Syst. Sci. Syst. Eng.*, 2004, **13**, (1), pp. 1–35

[21] Zhang H. and Li P: 'Probabilistic analysis for optimal power flow under uncertainty', *IET Gener. Transm. Distrib.*, 2010, **4**, (5), pp. 553–561

[22] Baradar M. and Hesamzadeh M. R.: 'A stochastic SOCP optimal power flow with wind power uncertainty'. Proc. *Proc. IEEE PES Gen. Meet.* 2014, pp. 1–5

[23] Blue Hill Observatory, 2014, URL: `http://www.bluehill.org/weatherdata`

[24] Detmers J.: *CAISO Operational Needs from Demand Response Resources*, CAISO, 2012, URL: `http://www.caiso.com/Documents`

[25] Grigg C. et al.: 'The IEEE reliability test system-1996. A report prepared by the reliability test system task force of the application of probability methods subcommittee', *IEEE Trans. Power Syst.*, 1999, **14**, (3), pp. 1010–1020

[26] Lofberg J.: 'YALMIP: A toolbox for modeling and optimization in MATLAB'. Proc. *Proc. IEEE CACSD*, 2004, pp. 284–289

[27] Smith J.: *Gurobi optimizer reference manual*, Gurobi Optimization, Inc., 2012, URL: `http://www.gurobi.com`